Optical Investigation of Low-Temperature Electric-Field-Induced Relaxations in Amorphous Solids

R. Wunderlich, H. Maier, and D. Haarer*

University of Bayreuth, D-95440 Bayreuth, Germany

B. M. Kharlamov

Institute of Spectroscopy, Russian Academy of Sciences, 142092, Troitsk, Moscow Region, Russia

Received: May 28, 1998

We have recently reported the optical detection of electric two-level system (TLS) dipoles in an organic polymer glass (*Phys. Rev. Lett.* **1995**, *74*, 5252). Here we present the results of more detailed investigations of electric properties of TLS in two-polymer glasses and a model description of the action of the external electric field. The influence of an external electric field on spectral diffusion (SD) in optical spectra of chromophores in organic amorphous solids at temperatures of 50−700 mK has been discovered and investigated via persistent hole burning. The field-induced spectral diffusion is caused by the interaction of the electric dipole moments of TLS with an external field. Electric field cycles disturb the equilibrium of the TLS ensemble. This causes an additional reversible diffusional broadening of spectral holes. A model description of the effect is presented, which is in quantitative agreement with the experimental results. The average values of the electric dipole moments of the TLS in two glasses, polymethylmethacrylate and polystyrene, are found to be on the order of 0.2 and 0.1 D, respectively. A modification of the hole-burning technique, based on the measurement of field-induced SD, is proposed that permits an increase of the time resolution of SD experiments far below the duration of the burning process. The investigation of the field-induced SD as a function of the field cycle time in the region of 1−300 min yields a slowly decreasing value of the TLS dipole moment with increasing cycle time. This effect points to a correlation between the dipole moments and the relaxation rates of TLS, which, to our knowledge, has not been observed before.

Introduction

At low temperatures, amorphous solids are characterized by anomalies of various properties like heat capacity, thermal conductivity, sound attenuation and velocity, optical line width of chromophores, etc. (see, for example, refs 1−3 and references therein). All these peculiarities are believed to result from the existence of a special kind of localized excitations—two-level systems (TLS). The main features of TLS dynamics arise from an extremely broad distribution of relaxation rates originating from their microscopic parameters represented by the energy asymmetry parameter Δ and the tunneling parameter λ as given in the standard TLS model.[2,4,5]

In spite of the great success of the TLS model in explaining experimental low-temperature properties of amorphous solids, the microscopic nature of TLS is still unclear. This is partially caused by the universality of TLS properties in very different materials; no clear correlations have, up to now, been found between the phenomenological TLS parameters and the microscopic physical or chemical nature of the investigated materials. Any information about the microscopic characteristics of TLS is therefore valuable for clarifying their atomic or molecular nature. One such parameter, which would yield valuable information for quantitative structural models,[6,7] is the electric dipole moment of a TLS. The existence of electric dipole moments causes an anomalous time and frequency behavior of the dielectric susceptibility. Starting from pioneering measurements of electric echoes in silica glasses,[8] some investigations of electric dipole properties in inorganic glasses were performed via electric methods.[9−11] With the exception of refs 12 and 13, no evidence for the existence of TLS dipoles in organic glasses has been obtained. In ref 13 their existence was demonstrated by the measurement of the high-frequency dielectric constant at low temperatures.

Another problem of the investigation of TLS dynamics is caused by the huge distribution of TLS relaxation rates, which has been experimentally proven to range at least from picoseconds to weeks.[3,15−23] There is no experimental technique that is able to cover the entire time regime. Different methods are used on different time scales, which makes it rather difficult to link and compare their results. But, as was recently shown,[22] the measurement of TLS dynamics in a very broad time range using a single experiment may provide basic new information about the TLS properties. Any improvements of existing experimental methods leading to an extension of their time ranges are therefore very valuable.

Since the first observation of persistent holes in organic glasses,[24] the hole-burning technique has been extensively used for the investigation of the low-temperature properties of amorphous solids (see, for example, the reviews in refs 25 and 26 and references therein). The phenomenon of spectral diffusion (SD)—the time evolution of the spectral line widths of chromophores in amorphous hosts due to TLS tunneling—renders persistent and transient optical hole burning very efficient tools for the investigation of TLS dynamics[3,21−23,25−30] at low temperatures. On one hand, persistent hole burning provides a unique technique for the measurement of ultraslow

10.1021/jp982411w CCC: $15.00
Published on Web 11/13/1998

TLS relaxations; recent experiments reached times up to 10^6 s[21−23] with no evidence yet for an upper boundary. But on the other hand, the lower bound of the time resolution of conventional persistent hole burning is limited by the time required for the burning process, which is usually of the order of 10 s (there are only few publications with better time resolution,[28−32] and as was noted in ref 30, even with a hole-burning quantum efficiency close to 100%, there is a serious problem of sample overheating by short burning pulses). Here, we propose a way to overcome this lower limit by utilizing the TLS electric dipole moments. Well after the creation of a spectral hole, fast TLS relaxations can be induced by switching an external electric field. The corresponding response of the spectral hole width can be observed on a time scale that is no more limited by the hole-burning process. Measurements with 50 ms time resolution are presented in this publication. Experiments with microsecond time resolution are in preperation.

Theoretical Aspects of Field-Induced Spectral Diffusion

General Considerations. In many cases, the phenomenon of SD in absorption spectra of impurities in amorphous hosts may be described qualitatively and even quantitatively in the frame of the standard TLS model.[33] But the classical approach only considers an ensemble of TLS in thermal equilibrium and therefore needs some modification for the nonequilibrium case. As a result of the very broad distribution of TLS relaxation times, ranging up to weeks with no evidence for an upper boundary, the TLS ensemble in the amorphous sample cannot reach a complete equilibrium even on such time scales after cooling. However, when the duration of an experiment is much shorter than the time interval between sample cooling and the beginning of the respective experiment, the TLS ensemble can be treated fairly well as being in equilibrium.[21,23] But there are of course situations where a nonequilibrium condition cannot be neglected. These are in particular experiments with time scales longer than the time interval between the sample cooling and the beginning of the experiment[21,23,34] and experiments with thermal cycles.[23,35] The first studies of nonequilibrium features of SD were described in refs 36 and 37 and continued in a more general way in refs 21, 23, 30, and 35.

The description of SD caused by an external electric field is formally very similar to thermal cycling. A first qualitative analysis of electric-field-induced nonequilibrium TLS dynamics was given in ref 14; a detailed description of the formalism will be presented here.

Nonequilibrium Extensions of the Standard TLS Model. The spectral diffusion kernel, i.e., the change of the hole width Γ in an amorphous host, is determined by the fraction $n(t_w)$ of TLS that have changed their state during the waiting time, t_w.[33]

$$\Gamma(t_w,T) \propto \left\langle \frac{\Delta}{E} n(t_w,T) \right\rangle_{E,\Delta_0} \tag{1}$$

Δ is the TLS energy asymmetry. It is connected with the respective energy via the relation

$$E = \sqrt{\Delta^2 + {\Delta_0}^2} \tag{2}$$

Δ_0 is the tunneling matrix element. The brackets denote an average over the distribution of the TLS parameters. The nonequilibrium features of SD enter into the variable n. Let us consider a subensemble of TLS with energy E_i in equilibrium at temperature T that has the following populations of the respective lower and upper states:

$$p_- = \frac{1}{(1+\exp(-E/k_BT))}; \quad p_+ = \frac{\exp(-E/k_BT)}{(1+\exp(-E/k_BT))} \tag{3}$$

If at $t = 0$ the energy splitting of the TLS ensemble instantaneously switches to E_f, it can be shown that the number of resulting transitions is given by

$$n(t_w,E_i,E_f,T) = n(E_i,E_f,T)\, f(t_w) = [p_+(E_i,T)\, p_-(E_f,T) + p_-(E_i,T)\, p_+(E_f,T)][1-\exp(-Rt_w)] \tag{4}$$

where $n(t_w,E_i,E_f,T)$ has been split up into a time-dependent and a time-independent part. $R = R(T,E_f,\Delta_0)$ denotes the relaxation rate of a TLS characterized by E_f and Δ_0. By insertion of p_+ and p_- from above, this formal expression can be evaluated to yield

$$n(E_i,E_f,T) = \frac{1}{2}\left[1 - \tanh\frac{E_i}{2k_BT}\tanh\frac{E_f}{2k_BT}\right] \tag{5}$$

It is useful to separate eq 5 into two expressions with different physical meanings:

$$\frac{1}{2}\left[1 - \tanh\frac{E_i}{2k_BT}\frac{E_f}{2k_BT}\right] = n_e + n_{ne} = \frac{1}{2}\left[\left(1 - \tanh^2\frac{E_i}{2k_BT}\right) + \tanh\frac{E_i}{2k_BT}\left(\tanh\frac{E_i}{2k_BT} - \tanh\frac{E_f}{2k_BT}\right)\right] \tag{6}$$

The first term on the right side reflects the equilibrium part of the TLS transition probability, e.g., for transitions with constant TLS energy E_i. The second term represents the additional probability, which comes into play due to the change of the TLS energy from E_i to E_f.

Now the mechanism of energy change under the action of an electric field $\vec{F}$ has to be specified. We will use the same simple approach as already given in ref 14. Every TLS possesses the same electric dipole moment. An application of an external electric field shifts the energy level of every TLS from its original value E_i to a value $E_f = E_i - \vec{\mu}\cdot\vec{F}$.[47] As a result of the random orientation of the electric dipoles relative to the external field, an orientational averaging has to be performed. After this averaging and with the substition $x = E_i/(2k_BT)$, the nonequilibrium part of the transition probability is given by

$$n_{ne}(x,F) = \tanh x\left[\tanh x - \frac{k_BT}{\mu F}\ln\frac{\cosh\left(x + \frac{\mu F}{2k_BT}\right)}{\cosh\left(x - \frac{\mu F}{2k_BT}\right)}\right] \tag{7}$$

Electric Field Cycling in a Time-Resolved Hole-Burning Experiment. Let us consider the time evolution of a spectral hole in an electric field cycling experiment. A hole is burned at $t = 0$ under equilibrium conditions. At $t = t_1$, an external electric field is switched on. As mentioned above, this shifts the energy splitting of every single TLS from its initial value E_i to $E_f = E_i + (\vec{\mu}\cdot\vec{F})$ and therefore instantaneously creates a nonequilibrium situation. At $t = t_2$, the field is switched off and the TLS ensemble evolves back to the initial equilibrium state with an energy splitting E_i. Here it is convenient to separate diffusional hole broadening into two contributions (equilibrium and nonequilibrium) according to the definitions

of eq 6; $\Gamma = \Gamma_e + \Gamma_{ne}$. There are three temporal stages in the time evolution of the spectral hole with different behavior of Γ_e and Γ_{ne}.

1. The Time Interval between Hole Burning and the Field Switching Time t_1. On the basis of eq 1 and using eq 6, one can readily obtain for Γ_e, the equilibrium part of the hole broadening.

$$\Gamma_e(T,t_w) = AT \int_0^\infty dx\, n_e(x) \int_0^{y_{max}} dy\, P(y)[1 - \exp(-R(x,T,y)\, t_w)] \quad (8)$$

where $y = \Delta_0/(2k_BT)$, $y_{max} = \min(x,\hbar\omega_0/(2k_BT))$, and $P(y)$ is the TLS distribution function in y. The standard model yields $P(y) = P_0/y$. As was shown earlier,[22] this function does not sufficiently describe the behavior of PMMA at low temperatures. We have found that in our experiments the best fit for equilibrium SD is provided by a distribution function proposed in ref 22.

$$P(y) = \frac{1}{y} + \frac{B}{y^2} \quad (9)$$

This phenomenological distribution function has found a theoretical interpretation in frames of a modified TLS model.[38,39] The deviations from the standard distribution function were observed not only in PMMA but also in proteins, both on long[40] and short[41] time scales. At the same time, the energy distribution of the standard model $P(E) = E/\Delta$ gives satisfactory results in our case.

At low temperatures, we need to take into account only first-order TLS−phonon interaction, which gives, for the TLS relaxation rate

$$R(T,x,y) = cy^2T^3x \coth x \quad (10)$$

As was shown earlier,[23] the internal integral in (8) can be solved analytically for the classical distribution function providing a logarithmic time dependence:

$$\int_0^{y_{max}} [1 - \exp(-R(x,T,y)\, t_w)] = \frac{1}{2}\{\gamma + \ln[R_{max}(T,x)\, t_w] + \mathrm{Ei}[R_{max}(T,x)\ t_w]\} \quad (11)$$

where Ei is an exponential integral, γ is the Euler constant, and $R_{max} = R(T,x,y_{max})$. If $t \gg 1/R_{max}$, the sum of the first and third terms approaches zero and only the logarithmic part survives. It is easy to evaluate the above integral analytically for the second part of distribution function (9).

$$\int_0^{y_{max}} \frac{B\, dy}{y^2}[1 - e^{-R(x,T,y)t_w}] = B\frac{\sqrt{\pi}\sqrt{R_{max}t_w}\,\mathrm{erf}(\sqrt{R_{max}t_w}) - 1 + \exp(-R_{max}t_w)}{y_{max}} \quad (12)$$

which transforms for $t \gg 1/R_{max}$ into

$$\int_0^{y_{max}} \frac{B\, dy}{y^2}[1 - e^{-R(x,T,y)t_w}] \approx \frac{B\sqrt{\pi}\sqrt{R_{max}t_w}}{y_{max}} \quad (13)$$

As a result of the limited time resolution in real experiments, it is impossible to measure the whole diffusional line width (the quantity that is measured is always a sum of homogeneous and diffusional line widths). The part of SD line broadening that may be measured is $\Delta\Gamma = \Gamma(T,t_w) - \Gamma(T,t_0)$ (t_0 in hole-burning experiments is limited by the hole-burning and registration time). Hence we have

$$\Delta\Gamma_e(T,t_w) \approx AT \int_0^\infty dx\, n_e(x)\left[\frac{1}{2}\ln\frac{t_w}{t_0} + \frac{B}{y_{max}}\sqrt{R_{max}(T,x)}(\sqrt{t_w} - \sqrt{t_0})\right] \quad (14)$$

In equilibrium conditions, the nonequilibrium contribution Γ_{ne} is zero.

2. Time Interval between t_1 and t_2, When the Field is Switched On. The expression for the equilibrium part of SD hole broadening remains the same (that is the advantage of separating SD into two parts), but a nonzero nonequilibrium contribution appears:

$$\Gamma_{ne}(t_w,t_1,T,F) = AT \int_0^\infty dx\, n_{ne}(x,F) \int_0^{y_{max}} dy\, P(y)\, \{1 - \exp[-R(x,T,y)\, (t_w - t_1)]\} \quad (15)$$

The time dependence of eq 15 is nearly the same as that of eq 8, only with the time origin shifted to t_1; therefore, the integration over y may be performed with a result similar to eq 14.

3. Time After Switching the Field Off ($t \geq t_2$). Again, the equation for Γ_e remains unchanged. Because the TLS ensemble was perturbed from its equilibrium in the previous time interval, the TLS populations are in a nonequilibrium state now, and therefore, the nonequilibrium part of the SD hole width remains nonzero. It is straightforward to obtain

$$\Gamma_{ne}(t_w,t_1,t_2,T,F) = AT \int_0^\infty dx\, n_{ne}(x,F) \int_0^{y_{max}} dy\, P(y)\, \{1 - \exp[-R(x,T,y)\, (t_2 - t_1)]\} \exp[-R(x,T,y)\, (t_w - t_2)] \quad (16)$$

It follows from eq 16 that the nonequilibrium part of SD hole broadening is reversible; $\Gamma_{ne} \to 0$ as $t_w \to \infty$. That fact is transparent in eq 16 with only the classical part of the distribution function ($P(y) = 1/y$). At $(t_w - t_2) \gg 1/R_{max}(x,T)$,

$$\Gamma_{ne}(T,t_w) \approx AT\frac{1}{2}\ln\frac{t_w - t_1}{t_w - t_2}\int_0^\infty dx\ n_{ne}(x) \quad (17)$$

Let us therefore note, in conclusion of this section, that the time evolution of the nonequilibrium part of SD hole broadening is governed by the same distribution function $P(y)$ as the equilibrium part. Therefore, the field-induced nonequilibrium SD may be used for measurements of the TLS distribution function in the same way as in the equilibrium case. But, there is a definite advantage; the experimental time resolution is not limited by the slow hole-burning process but only by the electric field switching time. Thus, a much higher time resolution may be reached than in conventional hole burning. This will be illustrated below.

Experimental Setup

^{3}He/^{4}He Dilution Refrigerator. An important part of our experimental setup is the optical ^{3}He/^{4}He dilution refrigerator.[42,43] The sample is placed directly into the dilute phase of the mixing chamber, which is built as a glass cylinder. This way an optimal thermal contact and a constant temperature of the sample are achieved via the superfluid ^{4}He. The optical scheme of the cryostat was described in detail in refs 42 and 43. Five windows and a heat reflection filter decrease the heat leak caused by room-temperature radiation to a value below 50

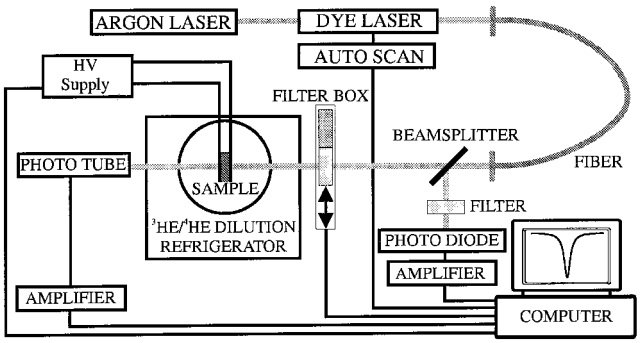

Figure 1. Experimental setup.

nW. The cooling power at 100 mK is 6 μW. The minimum temperature that can be reached is 24 mK. A very important advantage of this type of cryostat is a basically unlimited time of the cooling cycle (more than 100 days was experimentally achieved). It was reported that the nonequilibrium TLS dynamics has a great influence on the time behavior of persistent spectral holes, at least at temperatures below 1 K.[21,23,34] This effect is also observable in calorimetric experiments as a time-dependent heat release (see, for example, ref 47 and references therein). Therefore, to make sure that the sample is in thermal equilibrium, it is necessary to keep it at low temperatures long enough before starting measurements (for details see refs 21 and 23). We maintained the temperature of our sample below 1 K for 2 weeks before starting the first experiment, and we limited the duration of a single measurement to less than 4 h. Thermal nonequilibrium effects can be neglected under these conditions.[23]

Optical Setup. The optical setup of our experiment is presented in Figure 1. For burning and registration of the hole spectra we used a Coherent CR 699-29 Autoscan dye laser system. It consists of an actively frequency-stabilized single-mode ring laser with an integrated wavemeter. The estimated frequency jitter is below 2 MHz. The light was guided into the cryostat by a single-mode optical fiber. To suppress noise caused by fluctuations of the laser power and of the light polarization induced by the fiber, we employed a two-channel registration scheme; A polarization filter fixes the light polarization, and a beamsplitter divides the laser beam into two parts (reference and signal). The signal beam passes on its way to the cryostat a set of neutral density filters; the reference beam, attenuated by another set of neutral density filters, is registered by a photodiode. The transmission signal of the sample was normalized by the reference signal. This ensured an effective suppression of laser power and polarization fluctuations. The typical burning power at 100 mK was 0.5−1 μW, and the registration power was in the range of 100 pW.

Samples and Hole-Burning Conditions. Two kinds of polymers, polymethylmethacrylate (PMMA) and polystyrene (PS), were investigated. Both polymers were doped with tetraphenylporphin (TPhP). The optical density at the absorption maximum at 643 nm was $D = 0.8$ in the case of the PMMA samples and $D = 0.4$ in the case of PS samples. Three samples with different thicknesses in a range from 50 to 100 μm were placed between two ITO glass plates serving as electrodes. Because of the limited quality of the electric insulation of the wires used in our cryostat, the largest achievable voltage was 220 V in the first measurement series and 440 V after an improvement of the electric insulation. In the experiments, an initial voltage of $U = -400$ V was applied to the sample directly after cooling and all holes were burned under these conditions. The perturbation of the TLS equilibrium was performed by switching the voltage to values up to $U = +400$ V. A maximum field intensity of $F_{max} = 88$ kV/cm was reached in our measurements. The time constant of the field switching was 50 ms.

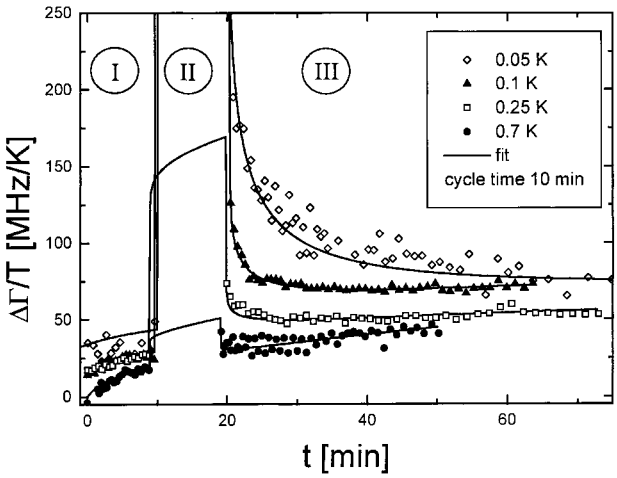

Figure 2. Temperature dependence of the field-induced nonequilibrium SD for a TPhP/PMMA sample. All measurements were carried out for a field change of $F = 88$ kV/cm during the field cycle. The hole broadening in all curves is normalized by the temperature. The solid lines are the fit curves (see text). The data sets are shifted with respect to each other to make them more distinguishable.

At 100 mK, the holes were burned with a typical burning energy of 10 μJ. The burning process took about 10 s. The relative hole depth was of the order of 10% with a half width of about 100 MHz (at 100 mK). The relative amplitude of the field-induced hole broadening is, even at the lowest temperatures, rather small; it is typically 10 MHz, 10% of the initial hole width. A reasonable signal-to-noise ratio in hole-broadening data was reached by averaging the results of a series of 15−30 measurements. The time resolution in the measurements of the hole profile after the field cycle was limited by the scanning time and was usually on the order of 10 s. To investigate TLS dynamics below 10 s, we measured the hole depth as a function of time after the electric field cycle. When a constant hole area (checked in control experiments) is assumed, the hole width is inversely proportional to the hole depth. In these measurements, the time resolution was only limited by the switching time constant of the high voltage.

Experimental Procedure and Results

Several series of measurements were performed on two samples of TPhP/PMMA and one sample of TPhP/PS. The procedure of the measurements was the same in all experiments. This procedure (corresponding to the scenario described in the theoretical section) is depicted in Figure 2. The spectral hole is burned, and its time evolution is monitored for 10−15 min (this time region is labeled as I in the figure). Then, the external electric field is switched to opposite polarity and the sample is kept in that state for a definite time (cycle time). The TLS ensemble is driven out of equilibrium at the time of the field switching, and it starts to evolve to the new equilibrium. This creates additional SD hole broadening, which is not observable due to the Stark effect of the chromophores (this time region is labeled as II). After the field is switched back to its initial value, the Stark effect disappears and the hole becomes observable again. The TLS ensemble, which was taken out of its equilibrium during the field switching cycle, now evolves back into its equilibrium. This is reflected by a hole narrowing (time

region III). This process contains information about the interaction between the TLS and the electric field. We investigated the dependence of field-induced SD on temperature, switching time, and the magnitude of the electric field.

As has been shown in the theoretical analysis (eq 7), the field-induced SD should be very sensitive to the sample temperature. Figure 2 shows this dependence in the temperature interval between 50 and 700 mK with a field-switching time of 10 min. All curves are normalized on the temperature in order to make the results comparable. The experimental data at 50 mK are measured on a different sample than the other three data sets. The typical features of the field-induced SD are clearly seen from the figure.

(1) The magnitude of field-induced SD relative to equilibrium SD decreases dramatically with increasing temperature. The relative amplitude of the field-induced SD is maximal at 50 mK, despite the fact that the absolute SD rate, decreasing linearly with temperature, is minimal at 50 mK. The effect practically disappears at 700 mK.

(2) As a result of the quasilogarithmic time behavior of the hole narrowing, the most dramatic change of the hole width takes place in the short time interval after the end of the field cycle and the amplitude of the measured effect strongly depends on the experimental time resolution (this point will be discussed later in more detail).

(3) The hole width after a field cycle asymptotically approaches the "unperturbed" limit, namely the width of the hole in an SD experiment without an electric field cycle (see also Figures 3 and 4). No observable evidence of irreversible broadening was obtained.

Thorough measurements of the dependence of the field-induced hole broadening on the amplitude of the electric field change were carried out. The goal was, in particular, to check for a possible influence of space charges, injected into the samples at high field intensities. If such processes take place, a small residual electric field remains in the sample even after the external field is switched off. That gives rise to some irreversible hole broadening caused by the Stark effect,[44] which can be time dependent due to a slow decrease of the concentration of space charges. As a result of the small amplitude of the field-induced SD in comparison with the Stark-induced hole broadening, the hole broadening induced by space charges could substantially disturb the SD effect. Despite of the fact that the field intensities in our experiments were an order of magnitude lower than those at which space charges were registered in similar samples,[44] we have checked their possible presence and can exclude it (see below).

Figure 3 summarizes the results of the investigation of the dependence of the nonequilibrium SD on the field intensity. Three sets of hole-broadening curves were obtained at different amplitudes of the electric field change (the field-switching time was 10 min in all measurements). It is clearly seen that the time dependence of the hole width is similar in all curves. The insert shows the fitted value of μF as a function of the field intensity F. The good linearity of the data set supports the applicability of our simple model.

Some additional checks for space charges were made; unipolar (from 0 to F) and dipolar (from $-^1/_2F$ to $+^1/_2F$) field switching was used in the experiments. It was found that the magnitude of the effect depends only on the difference between the field intensity before and during the field cycle and does not depend on the initial field value. Combining the results of temperature and field dependence measurements, we can conclude that no traces of space charges were detected.

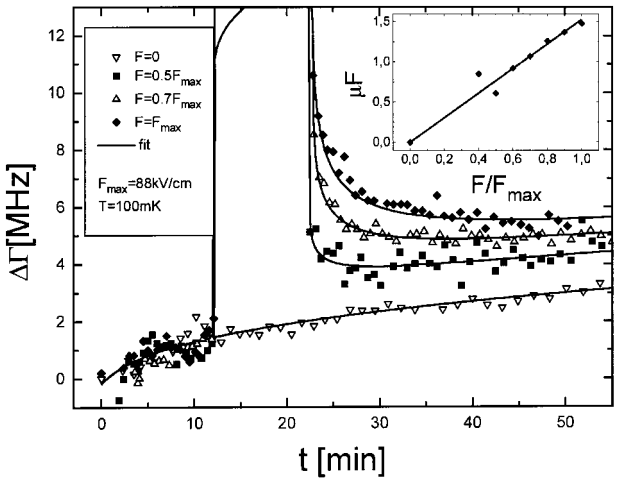

Figure 3. Dependence of the field-induced SD on the electric field intensity for the TPhP/PMMA sample. The temperature is 100 mK. The insert shows the dependence of the fitted value of μF on the field intensity.

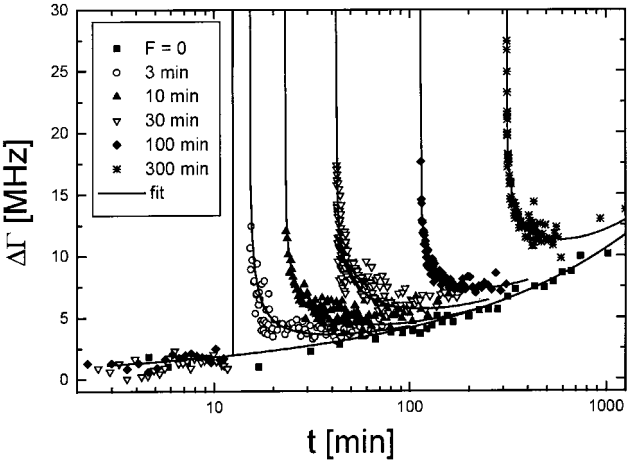

Figure 4. Dependence of the field-induced SD on the field-switching time. The sample (TPhP/PMMA) temperature is 100 mK.

The model calculations predict a quasilogarithmic dependence of the magnitude of the effect on the field-switching time (in the time scale of our measurements the "classical" part of the distribution function (9) dominates). We have investigated the influence of the field-switching time on the magnitude and time behavior of the field-induced SD on the PMMA samples at 100 mK in the range of 1−300 min. The results for switching times of 3−300 min are illustrated in Figure 4 (experiments with a switching time of 1 min were performed using a different measurement technique). With increasing field-switching time, not only the amplitude of deviation from equilibrium increases but also the duration of the "hole width recovery" period. These experimental observations coincide qualitatively with theoretical predictions, but the quantitative analysis shows some peculiarities, which will be discussed below.

As was pointed out in the theoretical section, the time resolution of the experiment is not limited by the hole-burning time and can easily be increased. In the present publication, we only demonstrate this possibility, measuring the field-induced effect with a time resolution of 50 ms. The results for a switching time of 1 min at a temperature of 50 mK are demonstrated in Figure 5.

This technique (hole depth measurement) only gives the relative hole broadening. The absolute values of hole widths were calculated using measurements of the hole profile before

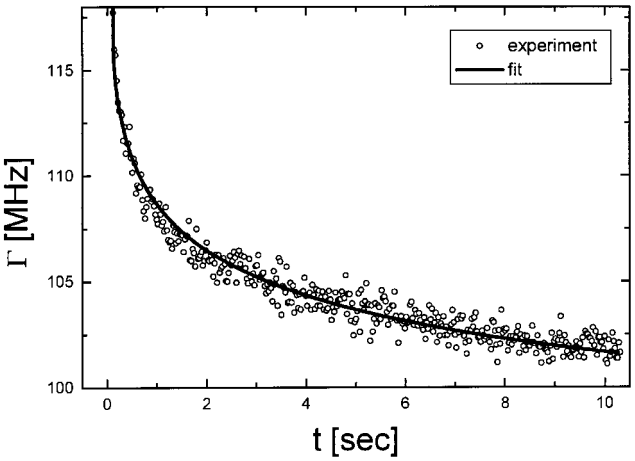

Figure 5. Results of the fast measurements of the field-induced SD at 50 mK. The field-switching time is 1 min.

the field cycle and in the long-time tail of the same measurement. As a result of better experimental statistics, the *S*/*N* ratio is better than in a "normal" series of measurements (All measured points are in the most sensitive part of the hole profile, namely on its top. By losing information about the hole profile, we gain in data acquisition rate). This makes the perspectives of a further increase of time resolution in field-switching experiments rather optimistic.

Discussion

Details of the Fitting Procedure. The above model description was well suited for fitting the experimental data. However, there is a coefficient that cannot be derived from our experiment directly, the TLS−phonon coupling constant c (see eq 10). The value of this constant was calculated based on literature data for TLS deformation potentials in PMMA.[45] Its literature value is $c \simeq 10^{10}\ \mathrm{K}^{-3}\ s^{-1}$. Actually, the results of the fit are not very sensitive to the value of that constant over a broad range. There are, in general, three fit parameters that can be obtained: A (see eq 8), which is proportional to the TLS−impurity coupling; B (see eq 9); the TLS electric dipole moment μ.

The first two parameters were derived from fits to experimental SD data without field cycle (the equilibrium SD was measured separately at all actual temperatures on time scales between a few hours and 1 week). Small complications appeared in these fits due to the measurable contribution of nonequilibrium effects in the low-temperature data (50−100 mK). That was unexpected, because the time interval between sample cooling and hole burning was in all experiments much longer than the time of the experiment itself. All our experiments, however, showed that the origin of this nonequilibrium effect is connected with light-induced SD.[46] The average value of A taken from many fits of equilibrium SD at temperatures of 50−700 mK was used for all fits of field-induced SD. For the coefficient B, we found that the best fits were obtained with a value of $B = k_b \times 10^{-7}$ K, which coincides with the value obtained earlier in experiments focussing on the long-time SD behavior on PMMA.[22] It should be pointed out that employing the standard TLS distribution function ($B = 0$) results in a rather bad fit of both equilibrium and field-induced SD. The source of that is quite clear from Figure 4: The hole-broadening curve without a field cycle ($F = 0$) is not a straight line in this semilogarithmic plot. That means even equilibrium SD in PMMA is evidently nonlogarithmic. It is very important to know as precisely as possible the equilibrium part of SD for an extraction of the field-induced nonequilibrium effect. That is the reason we used the modified TLS distribution function (9) in our fits of the equilibrium SD. We want to stress that the qualitative results are the same if the standard or modified TLS distribution function is used for data fitting, but the quantitative agreement between the model curves and experiment is much better in the latter case.

As follows from above the only free parameter in the fits of field-induced SD was the electric dipole moment of the TLS. The stability of this parameter in different experiments may be used as a criterion for the applicability of our model to real systems. Let us consequently analyze all experimental data under this aspect.

Temperature Dependence. The data at $T = 50$, 100, and 300 mK were obtained using one sample; another set of data at $T = 250$ and 700 mK was measured with another sample. We have compared the results obtained from one sample in order to avoid additional systematic errors caused by the error in the measurements of the sample thickness. The values of μ measured at different temperatures and at a field-switching time of 10 min coincide within 10%. It was already noted that at values of $\mu F \leq k_B T$ the amplitude of the effect decreases very fast. As a result of the finite breakdown strength of the samples, the electric field is limited to values below 10^6 V/cm; therefore, the field-induced SD is only observable in the subkelvin temperature region.

Dependence on Field Strength. The fit results of the TLS electric dipole moment measured at various field intensities are shown as an insert in Figure 3. The linearity of the data set illustrates the good stability of the fit results. The value of the electric dipole moment that is associated with the TLS and which was calculated from the slope of the fit line is 0.2 D (the discrepancy with the earlier reported value of 0.4 D[14] is connected with the relatively simple model description used in the first publication).

The dependence of the field-induced SD on temperature and field intensity also shows that the attribution of a constant dipole moment to every TLS is a rather good approximation. Another assumption was checked, $\mu \propto \Delta$. This assumption seemed to be the better model at first sight (symmetric TLS, for example, should have a zero dipole moment). But the model calculations based on this assumption lead to a much stronger field dependence of the SD than experimentally observed. Moreover, it can easily be shown that this assumption causes a field-induced SD that is temperature independent (of course only at low temperatures where $k_B T \ll \Delta_{max}$ is valid). This is in clear contradiction with experimental observations. That means the distribution of TLS dipole moments has no measurable correlation with the TLS asymmetry Δ. That result can be conceived as being in contradiction with experimental results measured via the dielectric echo technique. But our statement is not that there is no correlation at all. We have found only that the averaged (in the way specific for our experimental method) static electric dipole moment of TLS is not directly proportional to the averaged TLS asymmetry. A finite correlation should exist, but, with a high probability, the dispersion of electric dipole moments of TLS with the same asymmetry is so strong that this dispersion in the case of our measurement technique covers the above correlation.

Dependence on the Field-Switching Time. As was pointed out in the previous section, the time evolution of the field-induced SD coincides qualitatively with our model predictions. Quantitative agreement was also reached (see for example the fit curves in Figure 4), but the results display an unexpected

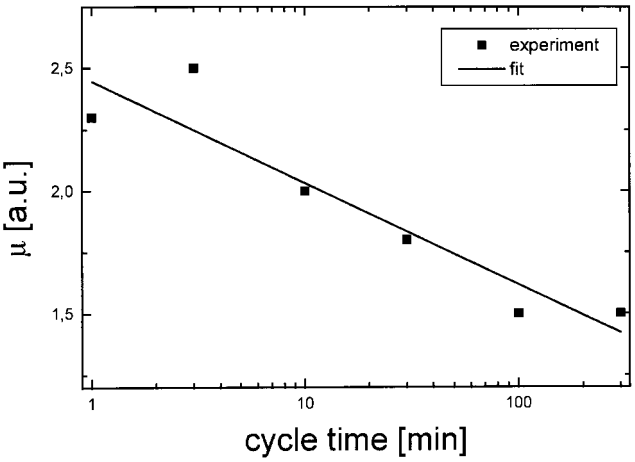

Figure 6. Dependence of the fitted value of the TLS electric dipole moment μ on the field-switching time.

tendency, the value of μ decreases systematically with increasing field-switching time. That result is demonstrated in Figure 6. The value of μ decreases approximately by 40% when the field-switching time is increased from 1 min to 300 min. This result is very stable relative to variations of the other fit parameters.

It is clear that not all TLS can possess equal dipole moments. In reality, their dipole moments should have a more or less broad distribution. This raises the question how this distribution should affect the experimental data. By decreasing the field-switching time, we exclude slow TLS from the relaxation process to the new equilibrium. The experiment is sensitive only for those TLS that can relax within the switching time. Therefore, the observed correlation of the averaged value of the TLS dipole moment with the field-switching time directly implies a connection between the dipole moment of a specific TLS and its relaxation rate. No information about such correlations has been found yet. Such a dependence may occur, for example, if the TLS size correlates with the relaxation rate. Large TLS should have a smaller dipole moment due to a better averaging of the charges in a big volume. This observation may shed some light onto the microscopic structure of TLS and open a new field for experimental and theoretical investigations of the microscopic properties of TLS.

Short-Time Measurement. As was pointed out above, the time resolution in the experiments with field-induced SD is not limited by the hole-burning time, the main limitation for short-time measurements in conventional hole-burning experiments. It is also clear that the short-time region is even more valuable due to the quasilogarithmic behavior of SD; in hole burning experiments, 5 decades in time were measured in a single experiment,[22] but in the short-time region, there are at least 10−11 orders of magnitude to be covered. It is very important to find a single experimental method that covers as much as possible of the entire time regime available. In principle, there are the following different experimental methods: two- and three-pulse photon echo in a time range of $10^{-12}-10^{-2}$ s and persistent hole burning in the range $10-10^{6}$ s. Here, we demonstrate a new technique of fast SD measurements with electric field cycles. The time resolution was increased with this technique by 2 orders of magnitude (relative to the resolution usually achieved in hole burning) and is now only limited by the time constant of the field switching. The experimental data were fitted with the same parameters and the same TLS distribution function as all other data. The results show that the quasilogarithmic hole-narrowing regime after the end of the field cycle continues in this time range. This means that by increasing the time resolution we can expect a monotonic increase of the amplitude of field-induced SD by approximately 10 MHz per decade. As we pointed out in the theoretical part, nonequilibrium SD is described by the same TLS distribution function as equilibrium SD, all salient features in this function (for example, gaps reported in ref 17) should also be observable in nonequilibrium SD dynamics if a proper time resolution can be achieved. We are now preparing measurements of field-induced SD with a time resolution on the order of 10 μs.

Polystyrene (PS) Samples. Qualitatively, the results obtained on PS samples are very similar to the ones on PMMA. But the resulting TLS electric dipole moment in PS of 0.1 D is 2 times smaller than the one in PMMA (which has more polar groups). This means that the electric dipole moments of the TLS are sensitive to the chemical composition of the polymer. Of course, more systems should be investigated in search of correlations between chemical structure and model parameters of the glasses.

Conclusion

We discovered and investigated in detail the influence of an external static electric field (EF) on the energy splitting of TLS caused by an interaction of the field with a parameterized electric dipole moment of the involved TLS. Any given change of the EF leads to a deviation of the TLS ensemble from equilibrium. This effect can be detected in optical hole-burning experiments by monitoring the time evolution of the spectral hole width. Electric-field-induced nonequilibrium SD leads to an additional hole broadening, which is reversible; the nonequilibrium component of the hole width asymptotically falls off to zero after the end of the electric field cycle.

A model description of the field-induced SD is presented. The dependence of the effect on temperature, field strength, and field-switching time is investigated and compared with model predictions. The model calculations agree quantitatively with the experimental results. The average values of the electric dipole moments of the TLS in two polymers, PMMA and PS, are measured. The time behavior of the field-induced nonequilibrium SD is governed by the same distribution function as the equilibrium SD. Therefore, not only the static electric dipole moments of TLS can be measured in experiments with electric field cycles but also the general properties of the TLS distribution function. The time resolution in these experiments is not limited by the hole-burning time, as in usual hole-burning studies. Therefore, this experimental technique allows an increase of the time resolution using persistent hole burning and field switching down to milliseconds and possibly microseconds. The investigation of the dependence of field-induced SD on a variation of the external conditions (temperature, field intensity, field cycle duration) leads to two new observations concerning the microscopic properties of TLS. (a) There is no direct correlation between TLS asymmetry and averaged static electric dipole moment. (b) There is a definite correlation between the TLS relaxation rate and the dipole moment; slow TLS have a smaller dipole moment.

The first observation is somehow surprising because it is usually assumed that the TLS dipole moment is proportional to the asymmetry. Possibly this correlation is covered by a broad distribution of electric dipole moments of TLS with the same asymmetry. The above results show that measurements of field-induced spectral diffusion open some new aspects for the investigation of low-temperature glass dynamics, which can hardly be achieved by means of traditional spectroscopy.

Acknowledgment. The work was supported by the Volkswagen Foundation (Grant No. AZ I/70 526), the part of the work performed in Russia was supported by the Russian Foundation of Basic Research (Grant No. 96-02-17566). The visit of one of the authors in Germany was supported by NATO Collaborative Research (Grant No. HTECH:CRG940406).

References and Notes

(1) Philipps, W. A., Ed. *Amorphous Solids*; Springer Verlag: Berlin, 1981.
(2) Phillips, W. A. *Rep. Prog. Phys.* **1987**, *50*, 1657.
(3) Friedrich, J.; Haarer, D. *Optical Spectroscopy of Glasses;* Zschokke-Gränacher, I., Ed.; Reidel: Dordrecht, 1986.
(4) Phillips, W. A. *J. Low Temp. Phys.* **1972**, *7*, 351.
(5) Anderson, P. W.; Halperin, B. I.; Varma, C. M. *Philos. Mag.* **1972**, *25*, 1.
(6) Heuer, A.; Silbey, R. *Phys. Rev. Lett.* **1993**, *70*, 3911.
(7) Dab, D.; Heuer, A.; Silbey, R. *J. Lumin.* **1995**, *64*, 95.
(8) Golding, B.; von Schickfus, M.; Hunklinger, S.; Dransfeld, K. *Phys. Rev. Lett.* **1979**, *43*, 1817.
(9) Röhring, V.; Saatkamp, T.; Kasper, G.; Hunklinger, S. *J. Non-Cryst. Sol.* **1989**, *107*, 166.
(10) Foote, M. C.; Golding, B.*Phys. Rev. B* **1991**, *43*, 9206.
(11) Höhler, R.; Menzel, J.; Kasper, G.; Hunklinger, S. *Phys. Rev. B* **1991**, *43*, 9220.
(12) Salvino, D. J.; Rogge, S.; Tigner, B.; Osheroff, D. D. *Phys. Rev. Lett.* **1994**, *73*, 268.
(13) von Schickfus, M.; Laermans, C.; Arnold, W.; Hunklinger, S. *Proceedings of the 4th International Conference on Physics of Non-Crystalline Solids*; Frischat, G. H., Ed.; Trans Tech: Dmansdorf, 1977.
(14) Maier, H.; Wunderlich, R.; Kharlamov, B. M.; Kulikov, S. G.; Haarer, D. *Phys. Rev. Lett.* **1995**, *74*, 5252.
(15) Small, G. J. Persistent nonphotochemical holeburning and the dephasing of impurity electronic transitions in organic glasses. In *Modern problems in condensed matter sciences*; Agronovich, V. M., Maradudin, A. A., Eds.; North-Holland: Amsterdam, 1983.
(16) Narasimhan, L. R.; Bai, Y. S.; Dugan, M. A.; Fayer, M. D. *Chem. Phys. Lett.* **1991**, *176*, 335.
(17) Meijers, H. C.; Wiersma, D. A. *Phys. Rev. Lett.* **1992**, *68*, 381.
(18) Gruzdev, N. V.; Vainer, Yu. G. *J. Lumin.* **1993**, *56*, 181.
(19) Schmidt, Th.; Macfarlane, R. M.; Völker, S. *Phys. Rev. B* **1994**, *50*, 15707.
(20) Zilker, S. J.; Haarer, D. *J. Chem. Phys.* **1996**, *105*, 10648.
(21) Maier, H.; Haarer, D. *J. Lumin.* **1995**, *64*, 87.
(22) Maier, H.; Kharlamov, B. M.; Haarer, D. *Phys. Rev. Lett.* **1996**, *76*, 2085.
(23) Fritsch, K.; Friedrich, J.; Kharlamov, B. M. *J. Chem. Phys.* **1996**, *105*, 1298.
(24) Kharlamov, B. M.; Personov, R. I.; Bykovskaja, L. A. *Opt. Comm.* **1974**, *12*, 191.
(25) *Persistent Spectral Hole Burning: Science and Applications*; Moerner, W. E., Ed.; Springer: Berlin, 1988.
(26) Orrit, M.; Bernard, J.; Personov, R. I. *J. Phys. Chem.* **1993**, *97*, 10256.
(27) Littau, K. A.; Bai, Y. S.; Fayer, M. D. *Chem. Phys. Lett.* **1989**, *159*, 1.
(28) Littau, K. A.; Dugan, M. A.; Chen, S.; Fayer, M. D. *J. Phys. Chem.* **1992**, *96*, 3484.
(29) Jahn, S.; Haarer, D.; Kharlamov, B. M. *Chem. Phys. Lett.* **1991**, *181*, 31.
(30) Kharlamov, B. M.; Jahn, S.; Haarer, D. *Opt. Spectrosc.* **1994**, *76*, 302.
(31) Wannemacher, R.; Smorenburg, H. E.; Schmidt, Th.; Völker, S. *J. Lumin.* **1992**, *53*, 266.
(32) Wannemacher, R.; Koedijk, J. M. A.; Völker, S. *Chem. Phys. Lett.* **1993**, *206*, 1.
(33) Reinecke, T. L. *Solid State Commun.* **1979**, *32*, 1103.
(34) Jahn, S.; Müller, K. P.; Haarer, D. *JOSA B* **1992**, *9*, 925.
(35) Khodykin, O. B.; Ulitsky, N. I.; Kharlamov, B. M. *Opt. Spektrosk.* **1996**, *80*, 489.
(36) Köhler, W.; Friedrich, J. *Europhys. Lett.* **1988**, *7*, 517.
(37) Littau, K. A.; Bai, Y. S.; Fayer, M. D. *J. Chem. Phys.* **1990**, *92*, 4145.
(38) Neu, P.; Reichman, D.; Silbey, R. *Phys. Rev. B.* **1997**, *56*, 5250.
(39) Heuer, A.; Neu, P. *J. Chem. Phys.* **1997**, *107*, 8686.
(40) Fritsch, K.; Eicker, A.; Friedrich, J.; Kharlamov, B. M.; Vanderkooi, J. M. *Europhys. Lett.* **1998**, *41*, 339.
(41) Störkel, U.; Creemers, T. M. H.; den Hartog, F. T. H.; Völker, S. *J. Lumin.* **1998**, *76*/*77*, 327.
(42) Müller, K. P., Ph.D. Thesis, University of Bayreuth, 1991.
(43) Müller, K. P.; Haarer, D. *Phys. Rev. Lett.* **1991**, *66*, 2344.
(44) Kador, L.; Haarer, D. *J. Appl. Phys.* **1987**, *62*, 4226.
(45) Federle, G., Ph.D. Thesis, Max-Plank-Institute of Solid State Physics Stuttgart, 1983.
(46) Wunderlich, R.; Maier, H.; Kharlamov, B. M.; Haarer, D. *Phys. Rev. B* **1998**, *57*, R5567.
(47) Formally it is more correct to use the following equation: $\Delta_f = \Delta_i - \vec{\mu}\vec{F}$. But, on the time scale of our experiment, the temporal evolution of the spectral diffusion (SD) is dominated by TLS with very low values of Δ_0 as compared with the average energy. Indeed, the average energy of the TLS in our experiments is about 0.1 K. We monitor the TLS dynamics with relaxation rates $r < 10\ s^{-1}$. The simple estimation, based on the known value of the coupling constant c in eq 10 gives for such TLS $\Delta_0 < 10^{-4}$ K. Therefore, in our case, for the majority of TLS it holds that $\Delta_0 \ll \Delta$, and thus Δ can be replaced with E, which simplifies the following analytical calculations.